Journal of Applied Mechanics and Technical Physics, Vol. 50, No. 6, pp. 1044–1048, 2009

ANALYSIS OF BIFURCATION BENDING MODES OF ARCHES AND PANELS

L. I. Shkutin

UDC 539.370

This paper reports the results of numerical analysis of the bifurcation solutions of nonlinear boundary-value problems of plane bending of elastic arches and panels. Problems are formulated for a system of six nonlinear ordinary differential equations of the first order with independent fields of finite displacements and rotations. Two loading versions (by follower and conservative pressures) and two versions of boundary conditions (rigid clamping and pinning) are considered. In the case of clamped arches and panels, the set of solutions consists of symmetric and asymmetric bending modes which exist only for positive values of the load parameter. In the case of pinning, the set of solutions includes symmetric and asymmetrical modes which correspond to positive, negative, and zero values of the parameter. In both problems, the phase relations between the state parameter and the load parameter are bifurcated, ambiguous, have isolated branches, and admit a catastrophe — a finite jump from the fundamental equilibrium mode to a buckled mode.

Key words: *arches, panels, nonlinear bend, buckling, stability, numerical analysis.*

With the development of computer facilities, the method of state parameter continuation for boundary-value problems has received extensive use in nonlinear structural mechanics [1, 2]. This method is used to find solutions bifurcating from the primary solution and requires special procedures for constructing solutions near bifurcation points. This makes it difficult to obtain isolated solutions characteristic of nonlinear deformation problems for rods, plates, and shells. In [3], the bending modes of an arch were analyzed and isolated branches of buckled modes were constructed by using a shooting method which reduces nonlinear boundary-value problems to a finite number of nonlinear Cauchy problems.

In the present work, some branches of unstable post-critical modes missed in [3] are constructed.

System of Equations. In Cartesian coordinates x_j with an orthonormalized basis $\boldsymbol{e}_j$ $(j = 1, 2, 3)$, the base line of length $2l$ of a circular arch (and a cylindrical panel) of radius r is given by the parametric equations

$$x_1 \equiv 0, \qquad x_2 = r(\cos(\alpha t) - \cos\alpha), \qquad x_3 = r\sin(\alpha t) \qquad \forall\, t \in [-1, 1],$$

where t is the internal parameter of the line and 2α is the angle of the arch. The arch has a constant section (profile) A, and the base line passes through its geometrical center. The plane bending of the arch under the load distributed along its length and specified (per unit length) by the vector $\boldsymbol{P} = P_2\boldsymbol{e}_2 + P_3\boldsymbol{e}_3$ is studied. It is required to find plane bending modes of the form

$$x_1 \equiv 0, \qquad x_2 = y(t), \qquad x_3 = z(t), \tag{1}$$

where y and z are the required functions. The material of the arch is considered transversally isotropic and linearly elastic.

Institute of Computational Modeling, Siberian Division, Russian Academy of Sciences, Krasnoyarsk 660036; shkutin@icm.krasn.ru. Translated from Prikladnaya Mekhanika i Tekhnicheskaya Fizika, Vol. 50, No. 6, pp. 155–160, November–December, 2009. Original article submitted December 8, 2008.

In the interval $(-1, 1)$, the nonlinear problem of plane bending is formulated as the system of six ordinary differential equations [3]

$$\begin{gathered} y_0' = y_1 + \alpha, \qquad y_1' = f_2 - (\gamma - 1)\varepsilon^2 f_2 f_3, \\ y_2' = \varepsilon^2(\gamma f_2 \cos y_0 - f_3 \sin y_0) - \sin y_0, \qquad y_4' = -p_2, \\ y_3' = \varepsilon^2(\gamma f_2 \sin y_0 + f_3 \cos y_0) + \cos y_0, \qquad y_5' = -p_3, \\ f_2 \equiv y_4 \cos y_0 + y_5 \sin y_0, \qquad f_3 \equiv -y_4 \sin y_0 + y_5 \cos y_0 \end{gathered} \tag{2}$$

with six unknown functions

$$y_0 = \theta, \quad y_1 = \frac{Yl}{H}, \quad y_2 = \frac{y}{l}, \quad y_3 = \frac{z}{l}, \quad y_4 = \frac{X_2 l^2}{H}, \quad y_5 = \frac{X_3 l^2}{H} \tag{3}$$

and parameters

$$\alpha = \frac{l}{r}, \quad \gamma = \frac{E}{G}, \quad \varepsilon^2 = \frac{I}{Al^2}, \quad p_j = \frac{P_j l^3}{H}, \quad H = EI. \tag{4}$$

In formulas (1)–(4), $y(t)$ and $z(t)$ are the required coordinates of the point t in the plane (x_2, x_3), $\theta(t)$ is the required angle of rotation about the x_2 axis, $Y(t)$ is the bending moment about the x_1 axis, $X_2(t)$ and $X_3(t)$ are the Cartesian components of the load vector, G is the transverse shear modulus, E is the longitudinal tension-compression modulus, and I is the moment of inertia of the cross section about the x_1 axis; prime denotes differentiation with respect to t.

System (2) describes the nonlinear elastic bending of the circular arch (and cylindrical panel) for specified values of the load parameters p_2 and p_3 and stiffness parameters α, γ, and ε, and specified boundary conditions.

Clamped Arch under Normal Pressure. Normal pressure is a follower load. Let P be the pressure intensity per unit length of the arch. In the bending state, the vector of the arch $\boldsymbol{P}(P_2; P_1)$ is directed normal to the base line (1), so that

$$P_2 = -P\cos\theta, \quad P_3 = -P\sin\theta, \quad p_2 = -p\cos y_0, \quad p_3 = -p\sin y_0. \tag{5}$$

In the numerical solution, the parameter $p = Pl^3/H$ was set constant (uniform pressure), and for $p > 0$ the vector $\boldsymbol{P}$ is directed along the inward normal. The conditions of rigid clamping of the arch at the boundary points (no rotations and displacements) are formulated as

$$y_0(\mp 1) = \mp\alpha, \qquad y_2(\mp 1) = 0, \qquad y_3(\mp 1) = \mp(1/\alpha)\sin\alpha. \tag{6}$$

The nonlinear boundary-value problem (2), (5), (6) was solved by a shooting method [3]. The main results of the numerical solution for an arch with parameters $\alpha = \pi/4$, $\gamma = 2.5$, and $\varepsilon = 0.02$ are presented in Fig. 1–4.

Figure 1 shows two branches of the curve of the state parameter q (displacements of the central point relative to the height of the arch) versus the pressure parameter p. (Positive values of p and q correspond to the load and displacement directed opposite to the x_2 axis.) Curve 1 is the branch of the lowest bending modes of the arch which are symmetric about the x_2 axis. The branch consists of three monotonic regions $1'$, $1''$, and $1'''$ and contains two critical points which are extreme for the dependence $p(q)$: the upper critical point with the coordinates ($p^+ \approx 18.500$; $q^+ \approx 0.157$) and the lowest critical point with the coordinates ($p^- \approx 4.50$; $q^- \approx 1.27$). Curve 2 (not found in [3]) is the branch of the lowest asymmetric modes which connects two bifurcation points of the first branch: the point with the coordinates ($p_B^+ \approx 15.000$; $q_B^+ \approx 0.067$) and the point with the coordinates ($p_B^- \approx 4.70$; $q_B^- \approx 1.17$). In the vicinity of the values p_B^+ and p_B^-, there are two equilibrium modes of the arch — symmetric and asymmetric. The equilibrium states corresponding to the points of the region $1'$ are commonly called the fundamental states, and the others the buckled states.

The possible equilibrium configurations of the clamped arch in the coordinates y/a and z/b (a is the height and $2b$ is the angle of the arch) at $p = 10$ are shown in Fig. 2. Curves $1'$, $1''$, and $1'''$ are symmetric modes that correspond to the points of the first branch. In the scale of Fig. 2, the fundamental mode $1'$ does not differ from the initial arch configuration, and $1''$ and $1'''$ are buckled modes. Curve 2 is a asymmetric buckled mode that corresponds to the point $p = 10$ of the second branch. All modes consist of three half-waves.

Figure 3 shows the strain distribution along the length of the clamped arch in three buckled states, and Figure 4 shows the parameter $Z = l^2 X_3/H$ (horizontal basic load) versus load parameter.

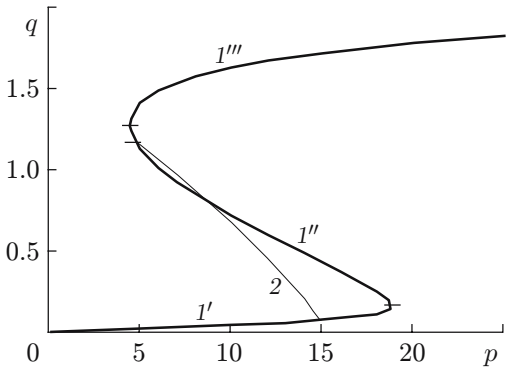

Fig. 1

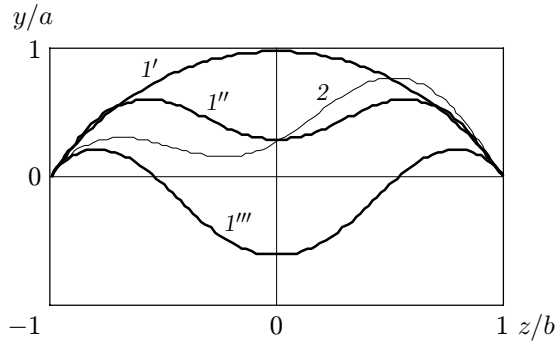

Fig. 2

Fig. 1. Bifurcation diagram of equilibrium states for the clamped arch under normal pressure: 1) branch of the lowest symmetric bending modes of the arch [segment 1 refers to the fundamental equilibrium states, segments $1''$ and $1'''$ refer to the buckled equilibrium states]; 2) branch of the lowest asymmetric bending modes of the arch.

Fig. 2. Equilibrium bending modes of the clamped arch under normal pressure ($p = 10$) (notation the same as in Fig. 1).

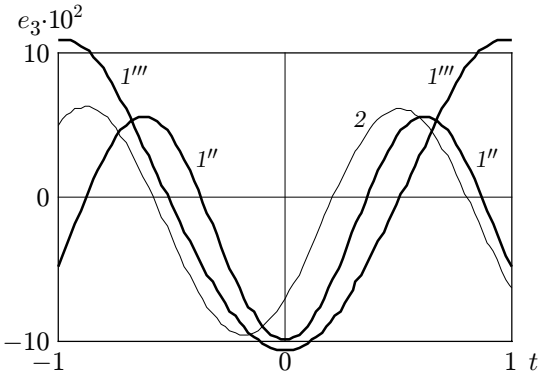

Fig. 3

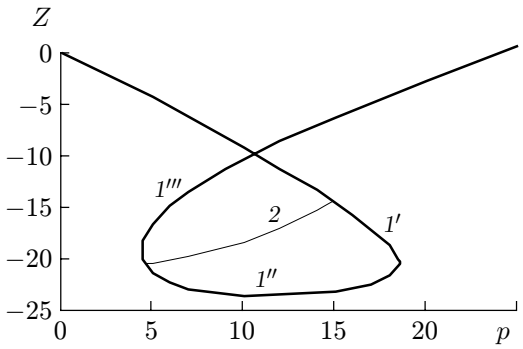

Fig. 4

Fig. 3. Strain distributions along the length of the clamped arch under normal pressure ($p = 10$) (notation the same as in Fig. 1).

Fig. 4. Evolution of the support reaction of the clamped arch under normal pressure (notation the same as in Fig. 1).

Pinned Arch under Gravity Pressure. The load of intensity P distributed uniformly on the arch and directed opposite to the axes x_2 will be called gravity pressure. During deformation, the vector $\boldsymbol{P}(-P; 0)$ moves translationally. The functions p_2 and p_3 in system (2) take values $p_2 = -p$ and $p_3 = 0$ ($p = Pl^3/H$ is the normalized pressure parameter). We consider the arch pinned at the boundary points so that at each of them, the conditions of no moments and displacements are satisfied:

$$y_1(\mp 1) = 0, \qquad y_2(\mp 1) = 0, \qquad y_3(\mp 1) = \mp(1/\alpha)\sin\alpha. \tag{7}$$

The nonlinear boundary-value problem (2), (7) was solved for an arch with the same parameters: $\alpha = \pi/4$, $\gamma = 2.5$, and $\varepsilon = 0.02$.

Figure 5 shows the results of calculation of three branches of the curve of the kinematic parameter q versus the pressure parameter p. Curves 1 and 2 are the branches of the lowest symmetric and asymmetric modes. The first branch (curve 1) has extreme critical points with the coordinates ($p^+ \approx 14.00$; $q^+ \approx 0.24$) and ($p^- \approx -6.7$; $q^- \approx 2.0$)

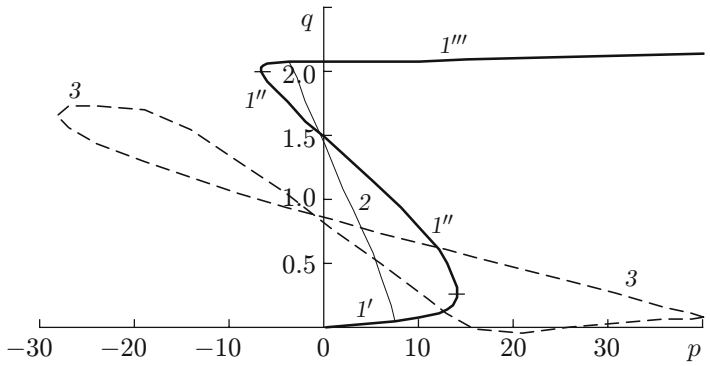

Fig. 5. Bifurcation diagram of equilibrium states for the pinned arch under gravity pressure: 1) branch of the lowest symmetric bending modes of the arch; 2) branch of the lowest asymmetric bending modes of the arch; 3) branch of the higher symmetric modes (notation the same as in Fig. 1).

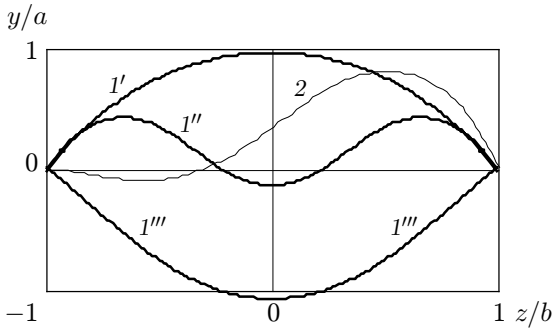

Fig. 6

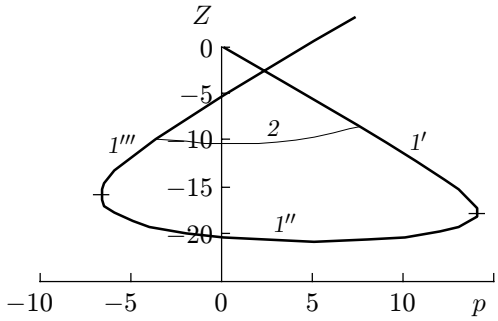

Fig. 7

Fig. 6. Equilibrium bending modes of the pinned arch under gravity pressure ($p = 5$) (notation the same as in Fig. 1).

Fig. 7. Evolution of the support reaction of the pinned arch under gravity pressure (notation the same as in Fig. 1).

and bifurcation points with the coordinates ($p_B^+ \approx 7.50$; $q_B^+ \approx 0.04$) and ($p_B^- \approx -3.7$; $q_B^- \approx 2.1$). The region of the first branch $1''$ not found in [3] is a set of unstable symmetric bending modes. The closed curve 3 contains the set of higher symmetric modes with three to five half-waves which are gradually transformed to one another [3].

Figure 6 shows possible configurations of a pinned arch at $p = 5$, and Fig. 7 the evolution of the supporting force parameter.

Conclusions. In the problems considered, the relations between the state parameter q and the load parameter p are bifurcated and ambiguous and admit a catastrophe — an instantaneous jump of the arch from the fundamental equilibrium mode to a buckled mode. Instability of the fundamental equilibrium modes due to small perturbations is most probable in the vicinity of the upper bifurcation load value. The stable symmetric configuration $1'$ is transformed to the unstable asymmetric configuration 2 and, in a jumpwise manner through the unstable symmetric configuration $1''$, it is transformed to the stable symmetric configuration $1'''$. The reverse jump to the branch $1'$ becomes possible at loads smaller than the lowest bifurcation value.

Along with the similarity of the bifurcation diagrams shown in Figs. 1 and 5, there is also a fundamental difference. Between the branches of the fundamental and buckled modes of the pinned arch there is an additional closed branch (curve 3 in Fig. 5). In addition, the pinned arch has a set of buckled modes for negative values of the load parameter and several modes for $p = 0$ that, in contrast to the initial arch configuration, are stressed and are counterbalanced by supporting forces.

The results obtained in [3] are supplemented by the construction of the branch of unstable asymmetric modes for the clamped arch (curve 2 in Fig. 1) and the branch of unstable symmetric modes for the pinned arch (curve $1''$ in Fig. 5). Thus, we obtained a complete bifurcation pattern for the solutions of the examined problems in the region between the branches of the fundamental and buckled modes.

Apart from the examined lowest bending modes, in [3] we constructed branches of multiwave solutions that exist at loads exceeding the upper extreme values. Such modes can result from shock loading of arches.

The results of the numerical analysis indicate that clamped arches are much more stable than pinned arches. This is due to the following factors: first, the upper bifurcation load of clamped arches is twice as high, and second, the set of values of the load parameter p for buckled modes has a positive lower bound.

The analysis of problems that admit free displacements of the boundary points along the x_3 axis (in this case, $y_5 \equiv 0$) leads to different results: the branches of the fundamental modes are monotonic, i.e., the possibility of a catastrophe is ruled out. On the contrary, a change in the nature of motion of the load (from translational to follower and back) does not bring qualitative changes to the solutions; moreover, the results are close quantitatively.

The results are valid for cylindrical panels with fixed rectilinear and free curvilinear edges.

This work was supported by the Russian Foundation for Basic Research (Grant No. 08-01-00148) and program of the Ministry of Education of the Russian Federation Development of Scientific Potential of Higher School (Grant No. 2.1.1/735).

REFERENCES

1. É. I. Grigolyuk and V. I. Shalashilin, *Problems of Nonlinear Deformation: The Parameter Continuation Method in Nonlinear Problems of Solid-State Mechanics* [in Russian], Nauka, Moscow (1988).
2. V. I. Shalashilin and E. B. Kuznetsov, "The best parameter for solution continuation," *Dokl. Ross. Akad. Nauk*, **334** No. 5, 566–568 (1994).
3. L. Shkutin, "Numerical analysis of the bifurcation forms of bending of arches," *J. Appl. Mech. Tech. Phys.*, **42**, No. 4, 310–315 (2001).